Separation Science and Technology
Publication details, including instructions for authors and subscription information:
http://www.informaworld.com/smpp/title~content=t713708471

Theory of Adsorption by Activated Carbon. I. Microscopic Aspects

David J. Wilson[a]; Ann N. Clarke[a]
[a] DepartmentS OF CHEMISTRY AND OF ENVIRONMENTAL, WATER RESOURCES ENGINEERING VANDERBILT UNIVERSITY, NASHVILLE, TENNESSEE

To cite this Article Wilson, David J. and Clarke, Ann N.(1979) 'Theory of Adsorption by Activated Carbon. I. Microscopic Aspects', Separation Science and Technology, 14: 3, 227 — 241
To link to this Article: DOI: 10.1080/01496397908066961
URL: http://dx.doi.org/10.1080/01496397908066961

SEPARATION SCIENCE AND TECHNOLOGY, 14(3), pp. 227–241, 1979

Theory of Adsorption by Activated Carbon. I. Microscopic Aspects

DAVID J. WILSON and ANN N. CLARKE

DEPARTMENTS OF CHEMISTRY AND OF
ENVIRONMENTAL AND WATER RESOURCES ENGINEERING
VANDERBILT UNIVERSITY
NASHVILLE, TENNESSEE 37235

Abstract

The adsorption of solutes by activated carbon is modeled at the microscopic level by means of the equations of continuity and mass balance. Two competing solutes are assumed present. The effects of the following parameters are considered: pore depth, radius, and variability of radius; solute diffusion constants; solute Langmuir isotherm parameters; and the rate constants for solute chemisorption. The results of this approach are then compared with a much simpler lumped parameter model for activated carbon adsorption of two competing solutes. Quite good agreement is obtained, which validates the utility of the simpler model.

INTRODUCTION

Although the use of chars as adsorbents for the removal of substances from gases and solutions dates back to the studies of Scheele and Lowitz in the late 18th century (*1*, *2*), this field continues to be a very active one for research and development. Hassler's book (*1*) provides an excellent introduction, discussion of a wide range of applications, and a large number of references. The Environmental Protection Agency has discussed in detail the use of activated carbon for the treatment of water and wastewater (*3*). DeBoer's monograph (*4*) provides a good treatment of the basic physical chemistry of adsorption processes generally, and gives very clear pictures of the physical models used and the magnitudes of many

of the relevant parameters. Keinath (*5*) has published a quite detailed discussion of the modeling of adsorption contactors by means of a lumped parameter approach, and has given computer programs for carrying out these calculations; he gives a number of useful references through 1972. Weber has given a detailed discussion of the application of activated carbon to water and wastewater treatment (*6*), including (among other topics) a discussion of solute diffusion in pores, continuous flow reactors, and design of fixed-bed contactors. Ying and Weber also recently presented some excellent work on biologically active beds of activated carbon (*7–9*); this includes some quite sophisticated mathematical modeling. Ford has recently tabulated the amenability of a large number of common organic compounds to activated carbon adsorption (*10*).

We are concerned here with the extent to which one can adequately model diffusion into a pore and Langmuir-type adsorption at a finite rate by means of a relatively simple and computationally tractable lumped parameter model. We determine this by carrying out computations on the adsorption of two competing solutes for a variety of systems by means of the two models.

ANALYSIS, FIRST MODEL

We consider the diffusion of solutes from a large reservoir of solution into a variable-diameter pore in a piece of activated carbon. We assume that the adsorption isotherms of the solutes are of the Langmuir type, and that the rates of increase in the surface concentrations of solute are first order in the solute concentrations and in the difference between the surface concentration and the surface concentration that is in equilibrium with the local concentration of solute in the solvent filling the pore.

The pores in activated carbon are not simple capillaries of constant diameter. We include the effects of variability of pore diameter r with distance from the mouth of the pore x by setting

$$r(x) = \frac{r_{\min} + r_{\max}}{2} - \frac{r_{\max} - r_{\min}}{2} \cos\left(\frac{2\pi x}{l_r}\right), \qquad 0 \le x \le l \qquad (1)$$

where $r_{\min}$ = minimum pore radius
$r_{\max}$ = maximum pore radius
l = pore depth
l_r = characteristic length associated with pore radius variation

We illustrate the model for a pore in Fig. 1.

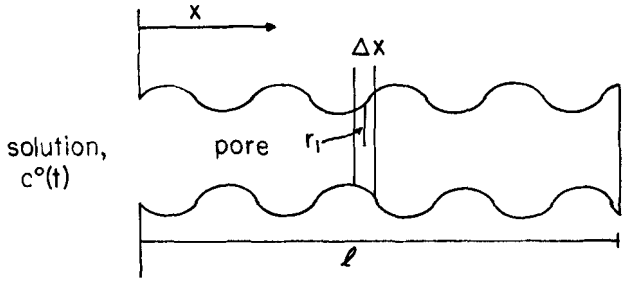

FIG. 1. Model for diffusion into a pore of variable diameter.

Since we use Langmuir adsorption isotherms, our coupled partial differential equations are nonlinear and require computer solution; we therefore develop the analysis from the beginning in terms of finite differences in the space coordinate. We assume that the approach of the solute surface concentrations $\Gamma_1(x, t)$ and $\Gamma_2(x, t)$ (moles/cm^3) to local equilibrium is given by

$$\frac{\partial \Gamma_i}{\partial t}(x, t) = k_i c_i(x, t)\{\Gamma_i^{eq}[c_1(x, t), c_2(x, t)] - \Gamma_i(x, t)\}, \qquad i = 1, 2 \quad (2)$$

where k_i is the rate constant for adsorption of the ith solute, and $\Gamma_i^{eq}[c_1, c_2]$ is the surface concentration of solute i in equilibrium with solution containing concentrations c_1, c_2 (moles/cm^3) of the solutes.

At local equilibrium we equate rates of adsorption and desorption to obtain

$$k_i c_i[1 - a_1\Gamma_1^{eq} - a_2\Gamma_2^{eq}] = k_i^r \Gamma_i^{eq}, \qquad i = 1, 2 \quad (3)$$

Here k_i and k_i^r are rate constants for adsorption and desorption, and a_i is the area (cm^2) occupied by 1 mole of solute i, assuming that the molecules are at the highest possible surface concentration.

From these equations we derive the following adsorption isotherm equations in the usual way:

$$\Gamma_1^{eq} = \frac{\Gamma_1^{max}}{1 + \dfrac{b_1}{c_1} + \dfrac{b_1 c_2}{b_2 c_1}} \quad (4)$$

$$\Gamma_2^{eq} = \frac{\Gamma_2^{max}}{1 + \dfrac{b_2}{c_2} + \dfrac{b_2 c_1}{b_1 c_2}}$$

where $b_j = k_j^r/k_j a_j$
$\Gamma_j^{max} = 1/a_j$

We are now ready to carry out a mass balance on the solution phase of the ith slab of Fig. 1. This yields

$$\frac{\partial c_j}{\partial t}(i, t)\pi r_i^2 \Delta x = \frac{\pi D_i}{4\Delta x}\{(r_i + r_{i-1})^2[c_j(i-1, t) - c_j(i, t)] + (r_i + r_{i+1})[c_j(i+1, t) - c_j(i, t)]\} - \frac{2}{r_i}\sqrt{1 + \left(\frac{dr}{dx}\right)_i^2}\,\pi r_i^2 \Delta x \frac{\partial \Gamma_j}{\partial t}(i, t) \tag{5}$$

The terms in braces are due to diffusion; the last term is due to mass transport between the liquid and surface phases and is obtained as follows. The total solute in the ith slab is given by

$$c_j(i, t)\pi r_i^2 \Delta x + \Gamma_j(i, t) \cdot 2\pi r_i \sqrt{1 + \left(\frac{dr}{dx}\right)_i^2}\,\Delta x \tag{6}$$

Since surface adsorption conserves mass, we can therefore write

$$\left(\frac{\partial c_j}{\partial t}\right)_{\text{surface ads}} \pi r_i^2 + \frac{\partial \Gamma_j}{\partial t} \cdot 2\pi r_i \sqrt{1 + \left(\frac{dr}{dx}\right)_i^2} = 0 \tag{7}$$

which yields

$$\left(\frac{\partial c_j}{\partial t}\right)_{\text{surface ads}} = \frac{-2}{r_i}\sqrt{1 + \left(\frac{dr}{dx}\right)_i^2}\,\frac{\partial \Gamma_j}{\partial t} \tag{8}$$

Multiplication of this by the volume of the ith slab yields the last term in Eq. (5).

Mass balances for the adsorbed solutes in the ith slab are obtained by combining Eqs. (2) and (4) to get

$$\frac{\partial \Gamma_1}{\partial t}(i, t) = k_1 c_1(i, t)\left\{\frac{\Gamma_1^{max}}{1 + \dfrac{b_1}{c_1(i, t)} + \dfrac{b_1 c_2(i, t)}{b_2 c_1(i, t)}} - \Gamma_1(i, t)\right\}$$

$$\frac{\partial \Gamma_2}{\partial t}(i, t) = k_2 c_2(i, t)\left\{\frac{\Gamma_2^{max}}{1 + \dfrac{b_2}{c_2(i, t)} + \dfrac{b_2 c_1(i, t)}{b_1 c_2(i, t)}} - \Gamma_2(i, t)\right\} \tag{9}$$

Equations (9) are substituted into Eq. (5) and the results rearranged to yield

$$\frac{\partial c_1}{\partial t}(i,t) = \frac{D_1}{4\Delta x^2 r_i^2}\{(r_i + r_{i-1})^2[c_1(i-1,t) - c_1(i,t)] + (r_i + r_{i+1})^2 \times [c_1(i+1,t) - c_1(i,t)]\} - \frac{2\sqrt{1 + (dr/dx)_i^2}}{r_i} k_1 c_1(i,t) \times \left\{\frac{\Gamma_1^{\max}}{1 + \dfrac{b_1}{c_1(i,t)} + \dfrac{b_1 c_2(i,t)}{b_2 c_1(i,t)}} - \Gamma_1(i,t)\right\}$$

$$\frac{\partial c_2}{\partial t}(i,t) = \frac{D_2}{4\Delta x^2 r_i^2}\{(r_i + r_{i-1})^2[c_2(i-1,t) - c_2(i,t)] + (r_i + r_{i+1})^2 \times [c_2(i+1,t) - c_2(i,t)]\} - 2\sqrt{1 + (dr/dx)_i^2} k_2 c_2(i,t) \times \left\{\frac{\Gamma_2^{\max}}{1 + \dfrac{b_2}{c_2(i,t)} + \dfrac{b_2 c_1(i,t)}{b_1 c_2(i,t)}} - \Gamma_2(i,t)\right\} \quad (10)$$

Equations (10) require modification at the ends of the pore, where $i = 1$ (mouth) and $i = N$ (bottom). The diffusion terms are the only ones affected; for $i = 1$ we have

$$\frac{\partial c_j}{\partial t}(1,t) = \frac{D_j}{4\Delta x^2 r_1^2}\{r_1^2[c_j^0(t) - c_j(1,t)] + (r_1 + r_2)^2[c_j(2,t) - c_j(1,t)]\} + \cdots, \qquad j = 1, 2 \quad (11)$$

and for $i = N$ we obtain

$$\frac{\partial c_j}{\partial t}(N,t) = \frac{D_j}{4\Delta x^2}\{(r_N + r_{N-1})^2[c_j(N-1,t) - c_j(N,t)]\} + \cdots, \qquad j = 1, 2 \quad (12)$$

Here $c_j^0(t)$ is the concentration of solute j in the bulk solution outside the pore, presumed known.

We integrate these equations forward in time by means of a standard predictor-corrector method of the following type.

$$\text{Starter: } y(\Delta t) = y(0) + \Delta t \frac{dy}{dt}(0) \quad (13)$$

$$\text{Predictor: } y^*(t + \Delta t) = y(t - \Delta t) + 2\Delta t \frac{dy}{dt}(t) \quad (14)$$

$$\text{Corrector: } y(t + \Delta t) = y(t) + \frac{\Delta t}{2}\left[\frac{dy}{dt}(t) + \frac{dy^*}{dt}(t + \Delta t)\right] \quad (15)$$

This algorithm is relatively fast and seems to be of quite high stability as the integration of the equations proceeds forward in time.

The total quantity of solute of type j contained within the pore is then given by the sum of the amount of dissolved solute and the amount of adsorbed solute:

$$M_j(t) = \sum_{i=1}^{N} [c_j(i, t)r_i^2 + 2\Gamma_j(i, t)r_i\sqrt{1 + (dr/dx)_i^2}]\pi\Delta x \qquad (16)$$

The first term gives the dissolved solute; the second, the adsorbed solute.

This approach gives us a quite realistic model of adsorption and diffusion within individual pores in activated carbon. Unfortunately, the model does not lend itself well to use for the description of activated carbon columns which are flow systems. In these one obtains even for a single-solute system a *very* large number of differential equations which must be integrated for a very long time in order to adequately describe the process. Basically, what one has, in essence, is a set of partial differential equations in three variables; time, distance down the column, and distance into the pore.

We therefore seek a simpler model for pore diffusion and adsorption which provides a description of these phenomena in good agreement with the more exact model analyzed above, but which makes much smaller demands for computer time. This is done as follows.

ANALYSIS, LUMPED PARAMETER MODEL

We approximate diffusion into the pore by a one-step process, as illustrated schematically in Fig. 2. Again we examine the case where two competing solutes are present, and we assume the same adsorption isotherms

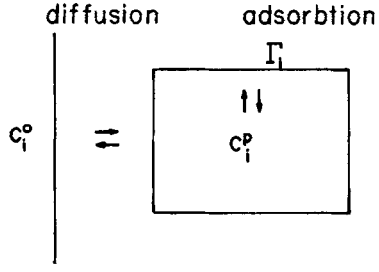

FIG. 2. Lumped parameter model.

and kinetics of adsorption as used for the first model, Eqs. (4) and (9). New notation is as follows:

v_p = volume of pore, $\pi r^2 l$ for a cylindrical pore
s_p = surface area of pore, approximately $2\pi rl$ for a cylindrical pore
A_p = effective cross-sectional area of pore, πr^2 for a cylindrical pore
D_j' = effective diffusion constant for solute j, a function of pore geometry as well as the identity of the solute; D_j' should vary as $2\alpha D_j/l$, roughly, for a cylindrical pore, where α is a constant of order unity
c_j^0 = bulk concentration of solute j
c_j^p = pore concentration (in solution) of solute j
Γ_j = surface concentration of adsorbed j

We note that conservation of solute during adsorption yields

$$v_p\left(\frac{\partial c_j^p}{\partial t}\right)_{\text{ads}} + s_p\frac{d\Gamma_j}{dt} = 0 \tag{17}$$

Material balance on component j in solution in the pore gives

$$v_p\frac{dc_j^p}{dt} = D_j'A_p(c_j^0 - c_j^p) + v_p\left(\frac{\partial c_j^p}{\partial t}\right)_{\text{ads}} \tag{18}$$

which, on use of Eq. (17), becomes

$$\frac{dc_j^p}{dt} = \frac{D_j'A_p}{v_p}(c_j^0 - c_j^p) - \frac{s_p}{v_p}\frac{d\Gamma_j}{dt}, \qquad j = 1, 2 \tag{19}$$

Our equations for Γ_1 and Γ_2 are essentially the same as before, with some obvious changes in notation:

$$\frac{d\Gamma_1}{dt} = k_1c_1^p\left\{\left[\Gamma_1^{\max}\Big/\left(1 + \frac{b_1}{c_1^p} + \frac{b_1c_2^p}{b_2c_1^p}\right)\right] - \Gamma_1\right\}$$

$$\frac{d\Gamma_2}{dt} = k_2c_2^p\left\{\left[\Gamma_2^{\max}\Big/\left(1 + \frac{b_2}{c_2^p} + \frac{b_2c_1^p}{b_1c_2^p}\right)\right] - \Gamma_1\right\} \tag{20}$$

We integrate these equations by the predictor-corrector method mentioned above. The total quantities of the two solutes within the pore are then given by

$$M_j(t) = s_p\Gamma_j(t) + v_pc_j^p(t), \qquad j = 1, 2 \tag{21}$$

The utility of this approach is determined by the extent to which the $M_j(t)$ calculated by Eq. (21) resemble those calculated by Eq. (16) from the more exact theory. One expects the diffusion constants in the two models to be quite different, but D'_j should be proportional to D_j/l; the parameters k_j, b_j, and Γ_j^{max} should be identical in the two models; and for a cylindrical pore one requires $v_p = \pi r^2 l$, $s_p = 2\pi rl$.

RESULTS

Computer programs were written to simulate activated carbon adsorption by means of the two models. A run simulating the first 200 sec of adsorption by means of the first model requires about 280 sec of computer time; a similar run using the lumped parameter model requires about 9.8 sec of XDS Sigma 7 computer time, about 1/29th the time required by the first model.

Figure 3 shows results for the two models for the case where the two

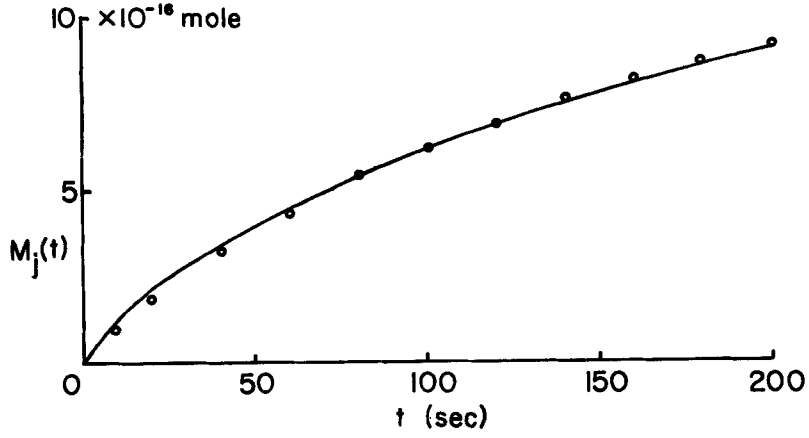

FIG. 3. Plots of $M_j(t)$ vs t for pore diffusion model (——) and lumped parameter model (○). Pore diffusion model parameters: $l = 5 \times 10^{-3}$, $r_{min} = 2 \times 10^{-4}$, $r_{max} = 2 \times 10^{-4}$, $l_r = 10^{-3}$ cm; $D_1 = D_2 = 10^{-7}$ cm²/sec; $\Gamma_1^{max} = \Gamma_2^{max} = 2 \times 10^{-10}$ mole/cm²; $b_1 = b_2 = 5 \times 10^{-9}$, $c_1^0 = c_2^0 = 10^{-6}$ mole/cm³; $k_1 = k_2 = 10^4$ cm³/mole sec; $\Delta t = 0.05$ sec; $N = 20$. Lumped parameter model: $s_p = 6.284 \times 10^{-6}$ cm²; $v_p = 6.284 \times 10^{-10}$ cm³; $D'_1 = D'_2 = 8.5 \times 10^{-5}$ cm/sec; $\Gamma_1^{max} = \Gamma_2^{max} = 2 \times 10^{-10}$ mole/cm²; $b_1 = b_2 = 5 \times 10^{-9}$, $c_1^0 = c_2^0 = 10^{-6}$ mole/cm³; $k_1 = k_2 = 10^4$ cm³/mole sec; $\Delta t = 0.05$ sec. $M_1^{eq} = M_2^{eq} = 12.55 \times 10^{-16}$ (dissolved 6.28, adsorbed 6.27) mole.

solutes are identical. The circles are the results of the lumped parameter model. D_1' was adjusted to give an optimum fit; the other parameters were assigned identical values for the two models. D_1'/D_1 is equal to 850, and the pore depth is 5×10^{-3} cm, so a reasonable value for α is 2.125. Except for the first few seconds, the agreement between the two models is astonishingly good. The initial discrepancy is due to the failure of the lumped parameter model to describe adequately the extremely rapid diffusion which occurs as a result of the very large concentration gradient at the mouth of the pore at the beginning of a run. These results indicate the utility of the lumped parameter model for dealing with single solutes.

We next examine the effect of changing the Langmuir isotherm parameters b_j; these are smaller the stronger the binding of the solutes to the surface of the activated carbon. The plots in Fig. 4 are for $b_1 = 2 \times 10^{-9}$, $b_2 = 5 \times 10^{-9}$ mole/cm^3. We find here slightly larger discrepancies between the two models. The lumped parameter model again fails to exhibit initial extremely rapid diffusion, and we also note that it shows too small a difference between $M_1(t)$ and $M_2(t)$ at later times. At very large times (not shown in the figure) the two models approach the same limiting values of $M_1(\infty)$ and $M_2(\infty)$, as one would expect. Figure 5, in which $b_1 = 2 \times 10^{-8}$, $b_2 = 5 \times 10^{-9}$ mole/cm^3, exhibits exactly

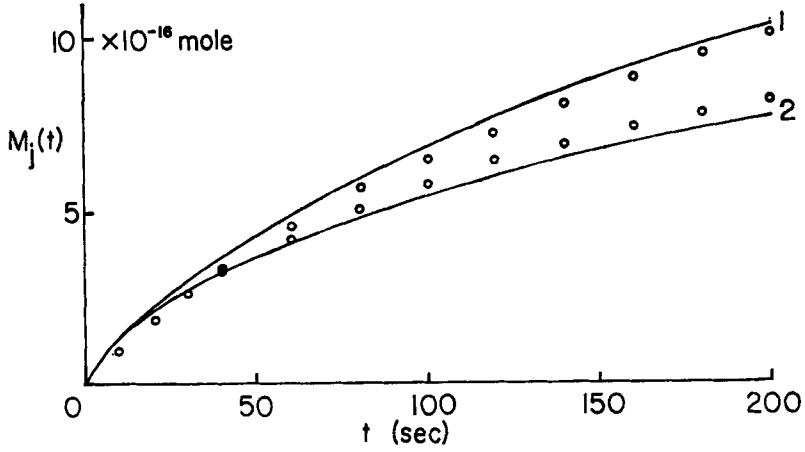

FIG. 4. Plots of $M_j(t)$ vs t for the two models; effect of b_j. $b_1 = 2 \times 10^{-9}$, $b_2 = 5 \times 10^{-9}$ mole/cm^3; other parameters as in Fig. 3. $M_1^{eq} = 15.25 \times 10^{-16}$ (dissolved 6.28, adsorbed 8.96), $M_2^{eq} = 9.87 \times 10^{-16}$ (dissolved 6.28, adsorbed 3.59) mole.

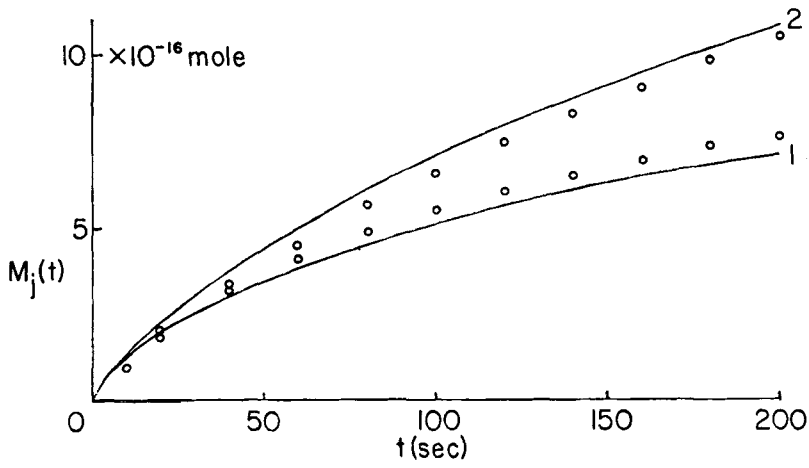

FIG. 5. Plots of $M_j(t)$ vs t for both models; effect of b_j. $b_1 = 2 \times 10^{-8}$, $b_2 = 5 \times 10^{-9}$ mole/cm^3; other parameters as in Fig. 3. $M_1^{eq} = 8.79 \times 10^{-16}$ (dissolved 6.28, adsorbed 2.50); $M_2^{eq} = 16.30 \times 10^{-16}$ (dissolved 6.28, adsorbed 10.01) mole.

the same effect. The diffusion constants D'_j in the lumped parameter model are the same as those in Fig. 3—no adjustments to improve fit were made in either Fig. 4 or Fig. 5.

The effect of pore length in increasing the time required to approach equilibrium is shown in Fig. 6. Here we plot the departure of $M_1(t)$ from its equilibrium value as a function of time for $l = 0.5 \times 10^{-3}$ and 10^{-3} cm. The linearity of the plots indicates that a single time constant is sufficient to describe most of the approach to equilibrium. The ratio of the slopes of the two plots is 2.0, confirming our earlier statement that D'_j in the lumped parameter model should be proportional to $1/l$.

The plots shown in Fig. 7 are for two solutes of differing diffusion constant; the results are pretty much what one would anticipate, with the more mobile solute approaching an equilibrium distribution in the pore more rapidly than the less mobile solute. The agreement between the pore model and the lumped parameter model is quite good; D'_1 and D_1 were both increased by a factor of 2, and no further adjustments in the parameters were made.

We see plots for two solutes having differing values of k_j, the rate constant for adsorption, in Fig. 8. The solute (1), which is more rapidly

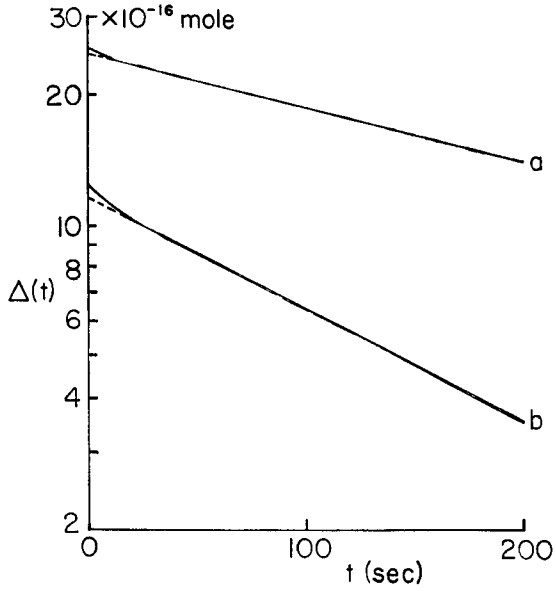

FIG. 6. Plots of $M_j^{eq} - M_j(t)$ vs t; effect of pore length in pore diffusion model. (a) $l = 10^{-2}$ cm. (b) $l = 5 \times 10^{-3}$ cm. Other parameters as in Fig. 3. Note that the ordinate is on a log scale.

adsorbed on the surface, equilibrates more rapidly than the solute which is less rapidly adsorbed (2), as one would anticipate. The lumped parameter model gives substantially less good agreement with the pore model for Solute 1 than for Solute 2; at present we have no explanation for this. Again, the values of D_j and D_j' used in Fig. 3 are employed without adjustment of D_j'.

Figures 9 and 10 exhibit the effects of varying the pore geometry. In both cases the pore radius oscillates between 1 and 2×10^{-4} cm; in Fig. 9 the distance over which this oscillation takes place is 10^{-3} cm, while in Fig. 10 this distance is 5×10^{-4} cm. The value of b_1 in both figures is 2×10^{-9} mole/cm^3; that of b_2, 5×10^{-9} mole/cm^3. The increased surface area of the pore in Fig. 10 results in greater adsorption of both solutes than is seen in Fig. 9. No attempt was made to compare these results with curves calculated from the lumped parameter model because of uncertainty as to what value of the effective cross-sectional area of the pore, A_p, should be used. The shapes of the curves are such, however,

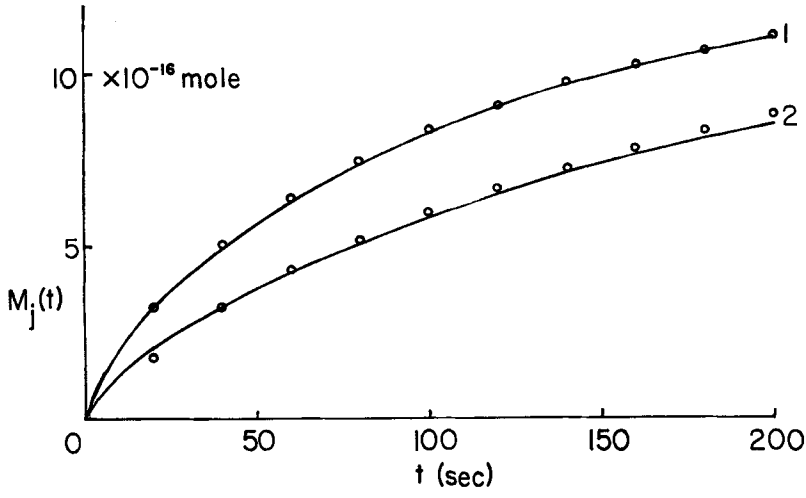

FIG. 7. Plots of $M_J(t)$ vs t for both models; effect of D_J. $D_1 = 2 \times 10^{-7}$, $D_2 = 10^{-7}$ cm^2/sec for pore diffusion model; $D_1' = 1.70 \times 10^{-4}$, $D_2' = 8.5 \times 10^{-5}$ cm/sec for lumped parameter model. Other parameters as in Fig. 3. $M_1^{eq} = M_2^{eq} = 12.55 \times 10^{-16}$ (dissolved 6.28, adsorbed 6.27) mole.

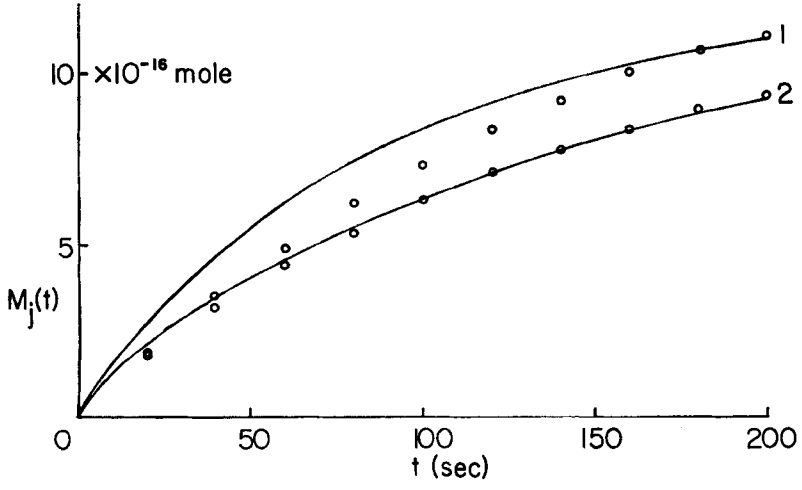

FIG. 8. Plots of $M_J(t)$ vs t for both models; effect of k_J. $k_1 = 5 \times 10^{-4}$, $k_2 = 10^{-4}$ cm^3/mole sec; other parameters as in Fig. 3. $M_1^{eq} = M_2^{eq} = 12.55 \times 10^{-16}$ (dissolved 6.28, adsorbed 6.27) mole.

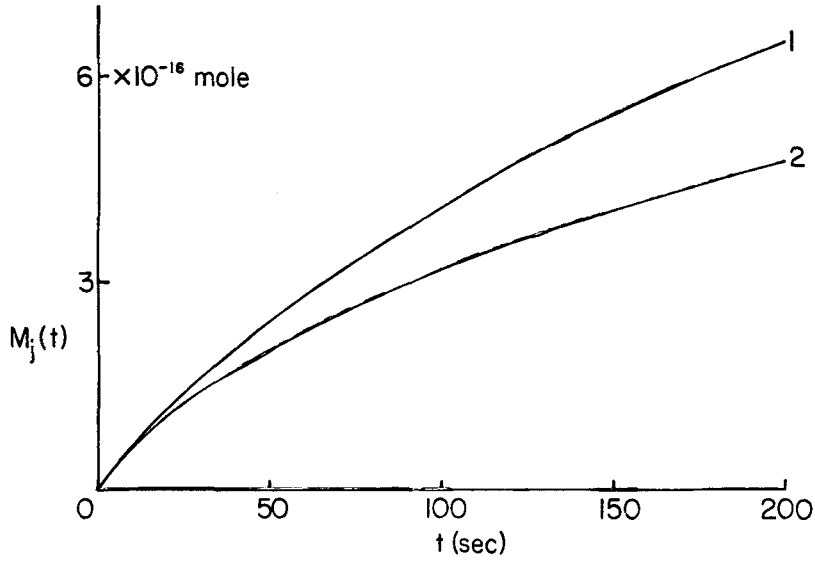

FIG. 9. Plots of $M_j(t)$ vs t for the pore diffusion model. Effect of varying pore diameter. $r_{min} = 10^{-4}$, $r_{max} = 2 \times 10^{-4}$ cm; $b_1 = 2 \times 10^{-9}$, $b_2 = 5 \times 10^{-9}$ mole/cm^3; other parameters as in Fig. 3. $M_1^{eq} = 10.62 \times 10^{-16}$ (dissolved 3.73, adsorbed 6.89); $M_2^{eq} = 6.49 \times 10^{-16}$ (dissolved 3.73, adsorbed 2.75) mole.

that we would anticipate little difficulty in adequately fitting lumped parameter model curves to these results by reasonable adjustments of the values of A_p.

We conclude that one can readily choose the constants in a lumped parameter model of adsorption of competing solutes by activated carbon to give rather good (but not perfect) agreement with the results of a highly realistic model of this process involving pore diffusion, Langmuir adsorption isotherms, and a finite rate of adsorption. The lumped parameter model calculations require about 1/29th the computer time required by the more exact model; this makes the lumped parameter model the one of choice in the modeling of continuous flow activated carbon columns. These models also apply to adsorption on other porous media such as alumina and silica gel.

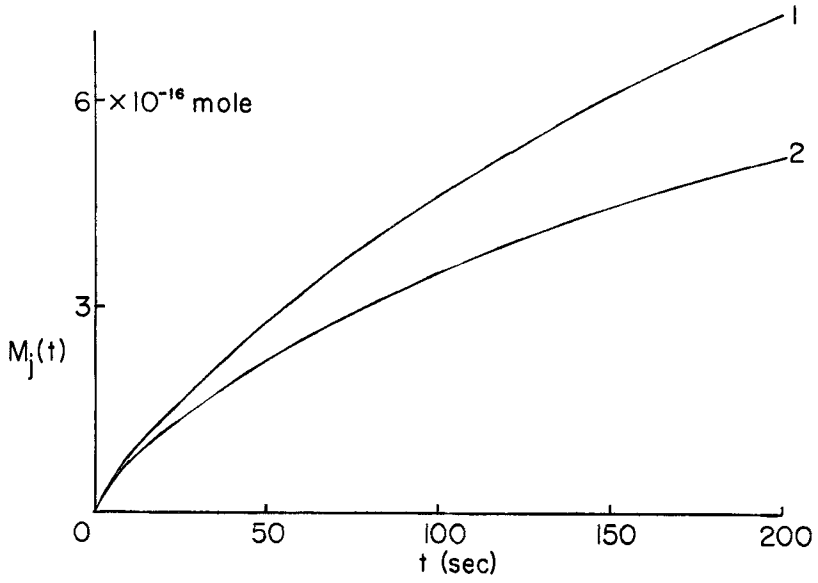

FIG. 10. Plots of $M_j(t)$ vs t for the pore diffusion model. Effect of varying pore diameter. $l_r = 5 \times 10^{-4}$ cm; other parameters as in Fig. 9, in which $l_r = 10^{-3}$ cm. $M_1^{eq} = 11.47 \times 10^{-16}$ (dissolved 3.53, adsorbed 7.94); $M_2^{eq} = 6.71 \times 10^{-16}$ (dissolved 3.53, adsorbed 3.18) mole. The increase in surface area in this pore as compared to that examined in Fig. 9 permits more adsorption.

Acknowledgment

This work was supported by a grant from the National Science Foundation.

REFERENCES

1. J. W. Hassler, *Purification with Activated Carbon*, Chemical Publishing Co., New York, 1974, Chap. 1.
2. W. D. Bancroft, *J. Phys. Chem.*, *24*, 127, 201, 342 (1920).
3. *Process Design Manual for Carbon Adsorption*, first revision, U.S. Environmental Protection Agency, Technology Transfer, October 1973.
4. J. H. deBoer, *The Dynamical Character of Adsorption*, Oxford, 1968.
5. T. M. Keinath, in *Mathematical Modeling for Water Pollution Control Processes* (T. M. Keinath and M. P. Wanielista, eds.), Ann Arbor Science Publishers, Ann Arbor, Michigan, 1975, Chap. 1.
6. W. J. Weber, Jr., *Physicochemical Processes for Water Quality Control*, Wiley-Interscience, New York, 1972, Chap. 5.

7. W. J. Weber, Jr., L. D. Friedman, and R. Bloom, Jr., "Biologically-Extended Physicochemical Treatment," in *Proceedings of the 6th Conference of the International Association for Water Pollution Research*, Pergamon, Oxford, 1973.
8. W. J. Weber, Jr., and W.-C. Ying, "Integrated Biological and Physicochemical Treatment for Reclamation of Wastewater," in *Proceedings of the International Conference on Advanced Treatment and Reclamation of Wastewater*, IAWPR, Johannesburg, South Africa, June 1977.
9. W.-C. Ying, "Investigation and Modeling of Bio-Physicochemical Processes in Activated Carbon Columns," Ph.D. Dissertation, The University of Michigan, 1978.
10. D. L. Ford, *Ind. Water Eng.*, p. 20 (May/June 1977).

Received by editor August 14, 1978